

Journal of Biomedical Optics

SPIEDigitalLibrary.org/jbo

Functional photoacoustic microscopy of diabetic vasculature

Arie Krumholz
Lidai Wang
Junjie Yao
Lihong V. Wang

Functional photoacoustic microscopy of diabetic vasculature

Arie Krumholz, Lidai Wang, Junjie Yao, and Lihong V. Wang

Washington University in Saint Louis, Optical Imaging Laboratory, Department of Biomedical Engineering, One Brookings Drive, St. Louis, Missouri 63130

Abstract. We used functional photoacoustic microscopy to image diabetes-induced damage to the microvasculature. To produce an animal model for Type 1 diabetes, we used streptozotocin (STZ), which is particularly toxic to the insulin-producing beta cells of the pancreas in mammals. A set number of ND4 Swiss Webster mice received intraperitoneal injections of STZ for five consecutive days at 50 mg/kg. Most mice developed a significant rise in blood glucose level (~ 400 mg/dL) within three weeks of the first injection. Changes in vasculature and hemodynamics were monitored for six weeks. The mouse ear was imaged with an optical-resolution photoacoustic microscope at a main blood vessel branch from the root of the ear. There are noticeable and measurable changes associated with the disease, including decreased vessel diameter and possible occlusion due to vessel damage and polyurea. We also observed an increase in the blood flow speed in the vein and a decrease in the artery, which could be due to compensation for the dehydration and vessel diameter changes. Functional and metabolic parameters such as hemoglobin oxygen saturation, oxygen extraction fraction, and oxygen consumption rate were also measured, but showed no significant change. © 2012 Society of Photo-Optical Instrumentation Engineers (SPIE). [DOI: 10.1117/1.JBO.17.6.060502]

Keywords: diabetes; photoacoustic microscopy; metabolism; streptozotocin; glucose.

Paper 12166L received Mar. 8, 2012; revised manuscript received Apr. 19, 2012; accepted for publication Apr. 20, 2012; published online May 21, 2012.

Photoacoustic tomography (PAT) is an emerging technology that generates high resolution, three-dimensional (3-D) images of the distribution of light-absorbing molecules, utilizing light-induced ultrasonic waves produced through the photoacoustic effect.¹ When imaging biological tissue, PAT techniques are sensitive primarily to optical absorbers, such as melanin, oxy-, and deoxy-hemoglobin.^{2,3} The sensitivity to hemoglobin in blood has yielded a new tool for many studies, including imaging the recovery of vessels after injury, and monitoring new vessel growth.⁴ The difference in color between arteries and veins results from the binding of oxygen to hemoglobin, changing the light absorption spectrum of the molecule. PAT can exploit this difference in the absorption to reveal functional information such as oxygen

saturation (sO_2). It has been shown that a spectral measurement of blood vessels using photoacoustic microscopy can yield a vessel-by-vessel map of the oxygen saturation in tissue.⁵ PAT is also capable of measuring the flow of blood in vessels, and the oxygen consumption rate in these tissues.⁶

Diabetes, characterized by excess glucose in the blood, is a risk factor for increasing retinopathy, renal failure, and cardiovascular disease.⁷ According to the American Diabetes Association, in 2011 there were 25.8 million children and adults with diabetes living in the United States, with 1.9 million new cases diagnosed annually in people aged twenty years and older. Optical-resolution photoacoustic microscopy (OR-PAM),⁸ one system implementation of PAT whose lateral resolution is determined by the optical focus, can measure diabetic vasculature and assist to better understand the physiologic changes induced by diabetes.

The OR-PAM system used in this study is shown in Fig. 1.⁹ This system's lateral resolution is defined by the tight illumination focus, with relatively loosely focused ultrasonic detection. The illumination light beam provided by a nanosecond-pulsed laser is focused through an optical lens and reflected off an aluminum-coated prism assembly, which reflects light but transmits sound, before striking the sample. The ultrasonic waves are focused by a 0.5 NA plano-concave acoustic lens and detected by a 50-MHz ultrasonic transducer (V214 BC, Olympus NDT). The signal is then amplified, digitized, and transferred to a computer. The whole imaging head—composed of the prism assembly, ultrasound transducer, and mounting frame—is raster-scanned to produce a 3-D image. The system scans with a voice-coil scanner in the x -direction, and with a stepper motor in the y -direction. A concurrent photodiode-reading compensates for fluctuations in the laser-pulse energy. The system resolution in the lateral direction is about $3.4 \mu\text{m}$, while the axial resolution is calculated to be around $15 \mu\text{m}$.

While there are many diabetes mouse models, the streptozotocin (STZ, Sigma) mouse model was chosen since it is inducible and inexpensive. STZ is specifically toxic to the beta cells of the pancreas, reducing the amount of insulin available to the animal; its administration is an established method for inducing insulin-dependent (type 1) diabetes in mice.¹⁰ PAT is particularly well-suited for measuring changes in diabetic vasculature because it can monitor vessel-by-vessel changes in diameter, sO_2 , blood flow speed, and total hemoglobin concentrations.

In this study, eight ten-week old male ND4 Swiss Webster mice, weighing approximately 30 g, were subjected to five consecutive intraperitoneal injections of an STZ solution. The injection concentration of 50 mg/kg in pH 4.5 citric buffer solution was sufficient to produce diabetes in the mice. The mice were subjected to food restriction for at least 6 h before injection. Using the OR-PAM system, each mouse was imaged around an artery and vein pair in the left ear. To monitor changes in total hemoglobin concentration and vessel diameter, the hemoglobin isosbestic point of 532 nm was used. To calculate the sO_2 , 532 and 561 nm wavelengths were used. Finally, each mouse was imaged for flow information with the method described previously.¹¹ Blood glucose was monitored using a glucometer (FreeStyle Lite®). Before administration of STZ, baseline measurements were acquired for all of the parameters.

After administration of STZ, blood glucose and body weight were monitored, and the mice were imaged once a week for six

Address all correspondence to: Lihong V. Wang, Washington University in Saint Louis, Optical Imaging Laboratory, Department of Biomedical Engineering, One Brookings Drive, St. Louis, Missouri 63130. Tel: +1 (314) 935-6152; Fax: +1 (314) 935-7448; E-mail: lhwang@wustl.edu.

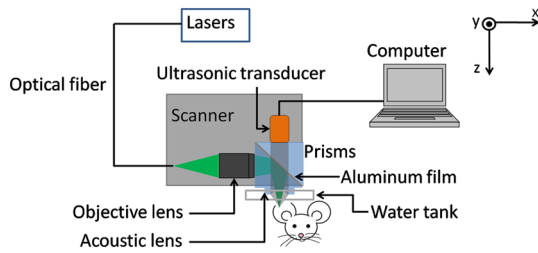


Fig. 1 System diagram for the optical-resolution photoacoustic microscope.

weeks to measure changes in vessel diameter, sO_2 , total hemoglobin, and blood flow speed. Within three weeks of administration of STZ, most mice developed a very significant rise in blood glucose level (from an average around 100 mg/dL to just under 400 mg/dL), which was indicative of severe uncontrolled diabetes.¹² Some representative results are shown in Fig. 2, with (a) showing the changes in the diameters of both the vein and artery in grayscale, along with the representative signal from the vessels, which is proportional to total hemoglobin concentration. Figure 2(b) shows the sO_2 calculated using a least-squares fitting method.¹³ The green dashed line in (a) represents the cross-section along which the flow measurements shown in Fig. 2(c) were taken. The flow results in Fig. 2(c) show a clear decrease in arterial flow speed and an increase in venous flow speed, as well as a clear decrease in vein diameter. Figure 2 is a representative data set of the mice tested. Four of the mice succumbed to complications from diabetes before the six weeks concluded.

The results for all the mice are summarized in Fig. 3, which shows a variety of effects stemming from the developing diabetes. Much literature on human and animal studies details the expected effects in the development of diabetes. Basically there is a balance between disturbance due to high glucose levels and the mouse's natural compensatory response to the adverse effects. As the blood glucose rose in the experimental mice [Fig. 3(a)], vessel diameter decreased in the arteries and more significantly in the veins [Fig. 3(b)], which can be explained by compensation for volume loss due to polyurea. In diabetic

polyurea, high blood glucose leaks into the urine and causes osmotic diuresis. Polyurea is responsible for the initial weight loss in the mice shown in Fig. 3(c).¹² The perfusion shown in Fig. 3(d) was considered to be the percentage of area filled with vessels in the imaged region excluding the main trunk vessels. This parameter was measured to test for changes induced initially by dehydration and subsequently by damage to the vessel walls by mechanisms still not well understood but related to the high blood glucose. However no significant change was observed.^{12,14} As Fig. 3(e) and 3(f) shows, there was no significant change in the sO_2 level in either the artery or the vein through the weeks, and there was also no significant change in the total hemoglobin concentration. The total hemoglobin concentration was calculated as the average signal from the artery and vein at an isosbestic wavelength; the concentration of hemoglobin at baseline was assumed to be 146 g/L on the basis of previous work.⁶

Presumably the metabolic demands of the mouse tissues remained at a similar level, at least at the onset of the disease. To compensate for the decreased vessel diameters, while still maintaining the same flux of oxygen and nutrients, blood flow speed must change correspondingly to maintain the volumetric flow rate. This trend is apparent in the results shown in Fig. 3(g). The oxygen delivered to the tissue can be estimated from blood flow, vessel diameter, and the oxygen extraction fraction (OEF). This fraction, shown in Fig. 3(h), is calculated to be the sO_2 in the artery minus the sO_2 in the vein, and the result is divided by the sO_2 in the artery. The O_2 consumption rate, shown in Fig. 3(i), takes into account the OEF, total hemoglobin concentration, and the flow rate; this parameter is calculated as discussed previously.⁶ The flow rates in the artery-vein pairs measured were the same within error at each of the weeks measured. In the mice measured, the calculated O_2 consumption rate in the measured tissue region did not significantly change through the weeks. The statistical analysis used was a one-way unbalanced ANOVA with a Tukey's multiple comparison test. In Fig. 3, the significance denoted for each week is in comparison to the baseline of each mouse.

These results show the feasibility of using PAM to monitor vascular changes associated with the sudden onset of

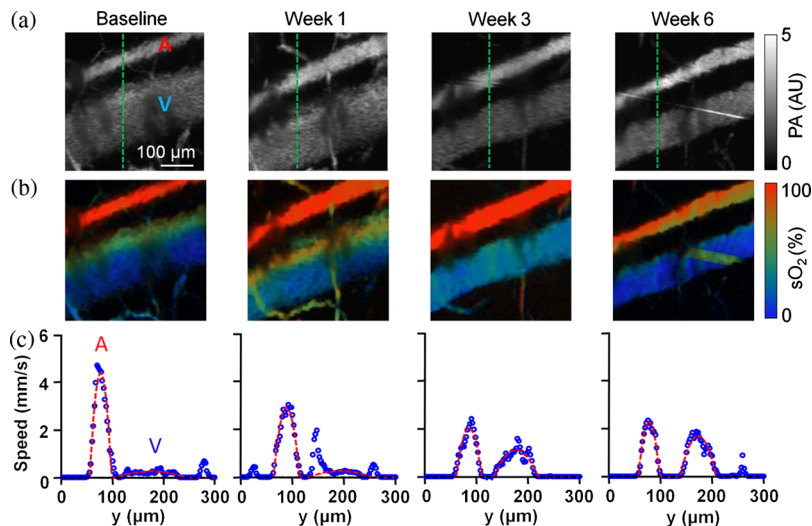


Fig. 2 Representative results for one streptozotocin-induced diabetic mouse showing (a) structural photoacoustic maximum amplitude projections (MAPs) through six weeks, (b) sO_2 MAPs of oxygen saturation in the main artery-vein pair studied, and (c) fitted flow speed profile through a cross section (green-dashed lines in panel a) of the main artery-vein pair. A: artery, V: vein.

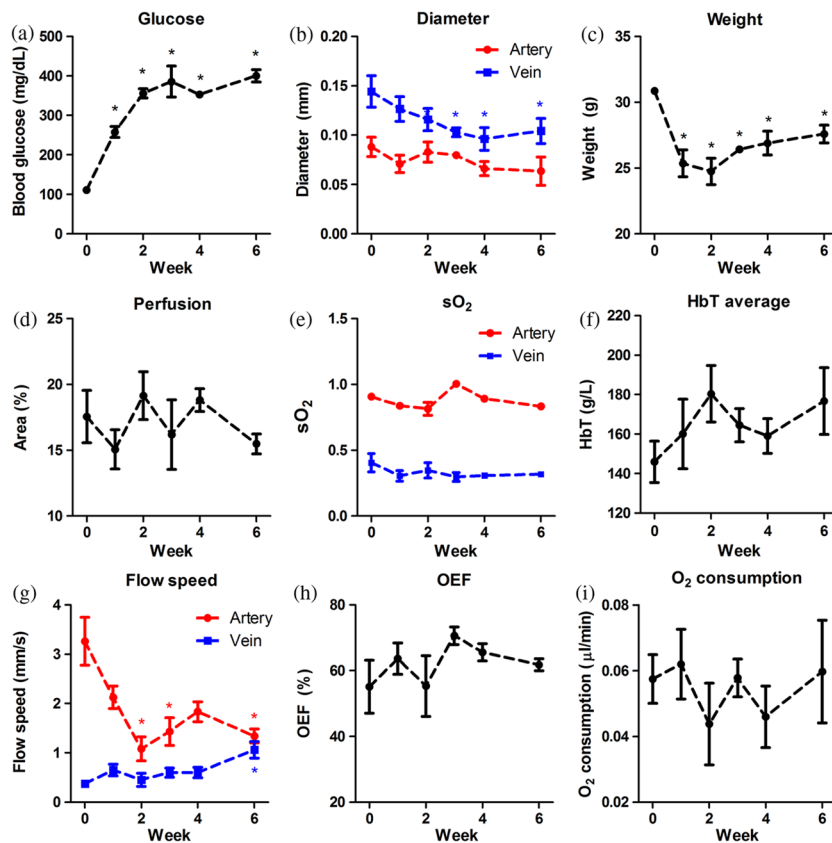


Fig. 3 Structural and functional changes from eight diabetic mice monitored for six weeks: (a) blood glucose concentration in mg/dl, (b) artery and vein diameters in mm, (c) mouse weight in grams, (d) perfusion in percent area, (e) sO_2 , (f) total hemoglobin concentration (HbT) in g/L, (g) flow speed in mm/s, (h) oxygen extraction fraction, and (i) oxygen consumption rate in $\mu\text{l}/\text{min}$. * $p < 0.05$, $n = 8$. Data are presented as means \pm s.e.m.

insulin-dependent diabetes in an STZ mouse model. There are noticeable and measurable changes associated with the disease, including decreased vessel diameter and possible occlusion due to vessel damage and polyurea. We also measured compensatory effects to maintain flow rate, and therefore nutrient delivery to the tissues, in the form of changes in the blood flow speed in the vessels, namely an increase in the flow speed in the vein and a decrease in the artery. Functional and metabolic parameters such as sO_2 , OEF, and O_2 consumption were also successfully measured, but showed no significant change. This study focused on the vascular and metabolic changes in acute onset severe uncontrolled insulin-dependent diabetes and clearly show morphological changes in the vasculature in the short-term period studied. Future studies will look into the long-term vascular changes in inducible models of noninsulin-dependent diabetes that would also improve animal survivability, as well as how treatment can affect the outcomes.

Acknowledgments

The authors thank Professor James Ballard for help with editing the manuscript. We would also like to thank Joel Schilling for training and information for the animal model. This research was funded by NIH grants: 5P60 DK02057933 R01 EB000712, R01 EB008085, R01 CA134539, R01 EB010049, U54 CA136398, R01 CA157277, and R01 CA159959. Lihong V. Wang has a financial interest in Microphotoacoustics, Inc. and Endra, Inc., which, however, did not support this work.

References

1. L. V. Wang, "Multiscale photoacoustic microscopy and computed tomography," *Nat. Photon.* **3**(9), 503–509 (2009).
2. L. V. Wang, "Prospects of photoacoustic tomography," *Med. Phys.* **35**(12), 5758–5767 (2008).
3. A. Krumholz et al., "Photoacoustic microscopy of tyrosinase reporter gene in vivo," *J. Biomed. Opt.* **16**(8), 080503 (2011).
4. S. Hu, K. Maslov, and L. V. Wang, "In vivo functional chronic imaging of a small animal model using optical-resolution photoacoustic microscopy," *Med. Phys.* **36**(6), 2320–2323 (2009).
5. H. F. Zhang et al., "Functional photoacoustic microscopy for high-resolution and noninvasive in vivo imaging," *Nat. Biotechnol.* **24**(7), 848–851 (2006).
6. J. Yao et al., "Label-free oxygen-metabolic photoacoustic microscopy in vivo," *J. Biomed. Opt.* **16**(7), 076003 (2011).
7. "Diabetes Statistics," American Diabetes Association, <http://www.diabetes.org/diabetes-basics/diabetes-statistics/> (2011).
8. K. Maslov et al., "Optical-resolution photoacoustic microscopy for in vivo imaging of single capillaries," *Opt. Lett.* **33**(9), 929–931 (2008).
9. L. Wang et al., "Fast voice-coil scanning optical-resolution photoacoustic microscopy," *Opt. Lett.* **36**(2), 139–141 (2011).
10. K. Honjo et al., "Histopathology of streptozotocin-induced diabetic DBA/2N and CD-1 mice," *Lab. Anim.* **20**(4), 298–303 (1986).
11. J. Yao and L. V. Wang, "Transverse flow imaging based on photoacoustic Doppler bandwidth broadening," *J. Biomed. Opt.* **15**(2), 021304 (2010).
12. A. C. Guyton and J. E. Hall, *Textbook of Medical Physiology*, 10th ed., W. Schmitt et al., Eds., pp. 894–895, Saunders, Philadelphia, Penn (2000).
13. H. F. Zhang et al., "Imaging of hemoglobin oxygen saturation variations in single vessels in vivo using photoacoustic microscopy," *Appl. Phys. Lett.* **90**(5), 053901 (2007).
14. N. Ruderman, J. Williamson, and M. Brownlee, "Glucose and diabetic vascular disease," *FASEB J.* **6**(11), 2905–2914 (1992).